

## Investigating neutron-proton pairing in $sd$ -shell nuclei via $(p, {}^3\text{He})$ and $({}^3\text{He}, p)$ transfer reactions

Y. Ayyad,<sup>1,2,\*</sup> J. Lee,<sup>3,4,†</sup> A. Tamii,<sup>1</sup> J. A. Lay,<sup>5,‡</sup> A. O. Macchiavelli,<sup>6</sup> N. Aoi,<sup>1</sup> B. A. Brown,<sup>7</sup> H. Fujita,<sup>1</sup> Y. Fujita,<sup>1</sup> E. Ganioglu,<sup>8</sup> K. Hatanaka,<sup>1</sup> T. Hashimoto,<sup>1</sup> T. Ito,<sup>1</sup> T. Kawabata,<sup>9</sup> Z. Li,<sup>10</sup> H. Liu,<sup>10</sup> H. Matsubara,<sup>11</sup> K. Miki,<sup>1</sup> H. J. Ong,<sup>1</sup> G. Potel,<sup>2</sup> I. Sugai,<sup>12</sup> G. Susoy,<sup>8</sup> A. Vitturi,<sup>5</sup> H. D. Watanabe,<sup>9</sup> N. Yokota,<sup>9</sup> and J. Zenihiro<sup>1</sup>

<sup>1</sup>Research Center for Nuclear Physics, Osaka University, Ibaraki, Osaka 567-0047, Japan

<sup>2</sup>National Superconducting Cyclotron Laboratory, Michigan State University, East Lansing, Michigan 48824, USA

<sup>3</sup>Department of Physics, The University of Hong Kong, Pokfulam Road, Hong Kong, China

<sup>4</sup>RIKEN Nishina Center, Wako, Saitama 351-0198, Japan

<sup>5</sup>Dipartimento di Fisica e Astronomia Galileo Galilei, Università di Padova and INFN, Sezione di Padova, via Marzolo 8, 35131 Padova, Italy

<sup>6</sup>Nuclear Science Division, Lawrence Berkeley National Laboratory, Berkeley, California 94720, USA

<sup>7</sup>Department of Physics and Astronomy and National Superconducting Cyclotron Laboratory, Michigan State University, East Lansing, Michigan 48824, USA

<sup>8</sup>Department of Physics, Istanbul University, Istanbul 34134, Turkey

<sup>9</sup>Department of Physics, Kyoto University, Kyoto 606-8502, Japan

<sup>10</sup>School of Physics and State Key Laboratory of Nuclear Physics and Technology, Peking University, Beijing 100871, China

<sup>11</sup>National Institute of Radiological Sciences (NIRS), Inage, Chiba 263-8555, Japan

<sup>12</sup>KEK, Oho 1-1, Tsukuba-shi, Ibaraki 305-0801, Japan

(Received 15 June 2017; published 23 August 2017)

Neutron-proton pairing correlations are investigated in detail via  $np$  transfer reactions in  $N = Z$   $sd$ -shell nuclei. In particular, we study the cross-section ratio of the lowest  $0^+$  and  $1^+$  states as an observable to quantify the interplay between  $T = 0$  (isoscalar) and  $T = 1$  (isovector) pairing strengths. The experimental results are compared to second-order distorted-wave Born approximation calculations with proton-neutron amplitudes obtained in the shell-model formalism using the universal  $sd$ -shell interaction B. Our results suggest underestimation of the nonnegligible isoscalar pairing strength in the shell-model descriptions at the expense of the isovector channel.

DOI: [10.1103/PhysRevC.96.021303](https://doi.org/10.1103/PhysRevC.96.021303)

The nucleon pairing phenomenon in atomic nuclei plays a crucial role in our understanding of many nuclear properties at low energy such as even-odd staggering in binding energies, moments of inertia, fission fragments charge distributions, and dynamics of spontaneous fission [1]. As in the Bardeen-Cooper-Schrieffer (BCS) theory of superconductors, neutron-neutron ( $nn$ ) and proton-proton ( $pp$ ) form strongly correlated pairs responsible for the appearance of such effects. Due to the short-range interaction between nucleons, neutrons and protons may couple to a correlated state with angular momentum  $J = 0$  and isospin  $T = 1$  (isovector or spin singlet). In nuclei with a large  $N - Z$  imbalance, the pairing interaction is essentially ruled by separated  $nn$  and  $pp$  correlations. Another channel to couple a neutron and a proton is the isoscalar (spin-triplet) mode with  $J = 1$  and  $T = 0$ , which is allowed under the Pauli principle.

In particular, for nuclei near the  $N = Z$  line, the protons and the neutrons have a large wave-function spatial overlap because the shell-model orbits for both of them are similar near the Fermi surface. In this case, the spin-triplet channel

interaction can become dominant, enabling the formation of  $np$  pairs. In addition, due to the charge independence of the nuclear force, pairing should manifest equivalently for the  $np$  pair with  $T = 1$  and  $S = 0$  and for the  $nn$  and  $pp$  [2]. Although the spin-triplet bare interaction is stronger than the spin singlet, there is widespread agreement that a strong nuclear spin-orbit interaction induces a stronger suppression of the former [3–5].

In spite of clear evidence of the  $np$  isovector mode  $T = 1$ , the existence of correlated isoscalar  $np$  pairs in condensate form and the magnitude of such collective pairings are still a controversial and fascinating topic that has renewed the interest in nuclear pairing. In particular, most of the current work conducted on this topic tries to elucidate the interplay between the isoscalar and isovector  $np$  modes and the possible transitions (and possible mixing configurations) between them.

From the theoretical point of view, the  $np$  pairing and the interplay between both modes have been extensively studied using different approaches and formalisms, mainly based on shell-model and mean-field calculations. The earliest research efforts on  $np$  pairing were devoted to extending the Hartree-Fock-Bogoliubov theory to include isovector and isoscalar pairing modes (see Ref. [6] and references therein). In these early works, for  $N = Z$  and  $N > Z$  even-even nuclei with  $A < 50$ , the isoscalar and isovector pairing modes appear, respectively, in the ground state. More recently, the Hartree-Fock-Bogoliubov theory was applied by Bertsch and Luo [5] to investigate the competition between isoscalar and isovector pairing in nuclei with  $A > 100$ . They concluded that

\*Present address: Nuclear Science Division, Lawrence Berkeley National Laboratory, Berkeley, California 94720, USA; ayyad@lbl.gov  
†jleehc@hku.hk

‡Present address: Departamento de Física Atómica, Molecular y Nuclear, Facultad de Física, Universidad de Sevilla, Apartado 1065, 41080 Sevilla, Spain.

spin-triplet pairing would dominate in  $N = Z$  nuclei with at least  $A \sim 130\text{--}140$ , a region close to the drip line. Using a many-body model described by Bogoliubov–de Gennes equations and the same Hamiltonian as in Ref. [5], Gerzelis, Bertsch, and Luo [7] found that the condensate is a mixture of spin-singlet and spin-triplet pairing, which appears when there is a large  $N-Z$  imbalance, close to the proton drip line. By examining the pairing vibrations around  $^{56}\text{Ni}$ , Macchiavelli *et al.* [8], confirmed the collective behavior of the isovector pairing vibration. However, their results do not support any manifestable collectivity of the isoscalar mode. Later, Yoshida [9] demonstrated that low-lying  $1^+$  states in odd-odd  $N = Z$  nuclei can be a precursory soft mode of the  $T = 0$  pairing condensation. In his Skyrme–energy density functional framework, the strong collective nature of the  $T = 0$   $np$  pairing vibrational may enhance the  $np$  transfer strength to the  $1^+$  state. This enhancement of the  $np$  transfer over the single-particle strength was previously pointed out by Fröbich [10] and, more recently, by Van Isacker and collaborators [11] within the interacting boson model. As with the case of  $(t, p)$  and  $(p, t)$  reactions, the experimental measurement of an  $np$  pair transfer would constitute one of the most adequate probes for understanding pairing correlations. The addition of particles in the system will introduce a transition to a pair condensate ground state for nuclei far from closed shells. In that superfluid region, cross sections are rather constant and enhanced by a factor  $\Omega^2$ ,  $\Omega$  being the single-particle degeneracy. It therefore seems natural to perform  $np$  pair transfer reactions on odd-odd self-conjugate nuclei, especially for heavier systems with larger single-particle degenerancies  $\Omega$ .

In this work, we performed  $(p, ^3\text{He})$  and  $(^3\text{He}, p)$  transfer reactions in  $N = Z$   $sd$ -shell nuclei to quantify the nature and interplay between  $T = 0$  ( $J = 1$ ) and  $T = 1$  ( $J = 0$ ) pairing correlations. Since  $\Delta T = 0$  and  $\Delta T = 1$  are allowed in these reactions, the exclusive cross sections to the lowest  $0^+$  and  $1^+$  states in odd-odd  $N = Z$  nuclei can be measured. Although several of these reactions were previously investigated [12–14], the measurements were performed under different experimental conditions by several groups over a number of years. For almost all of these previous measurements, no cross-section data were obtained at forward angles, where the effect of the addition of the  $L = 2$  component is minimum in the case of the  $0^+$ -to- $1^+$  transition. In our experiment, we measured the differential cross sections covering an angular range from close to  $0^\circ$  up to  $30^\circ$  to disentangle the  $L = 0$  and  $L = 2$  contributions. We obtained the ratio of the cross sections  $\sigma(0^+)/\sigma(1^+)$ , which provides a model-independent measurement of the  $T = 1/T = 0$  interplay and of the pairing collectivity [2,15]. Moreover, absolute cross sections are essential to determine the dynamical implications of  $T = 0$  and  $T = 1$ . Coupled with theoretical structure and reaction studies, a quantitative comparison between these measurements and theoretical cross sections is presented. Our work provides an essential framework for evaluating the microscopic descriptions of  $np$  pairing correlations in many-body wave functions and serves as the foundation for systematic studies of  $np$  pairing along  $N = Z$  nuclei via cross-section measurements. These newly improved systematic measurements under the same experimental conditions will provide an independent

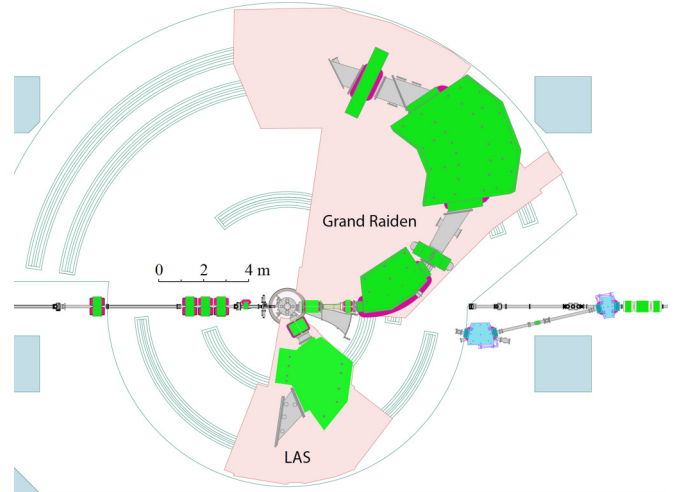


FIG. 1. Sketch of the Grand Raiden spectrometer and the large acceptance spectrograph (LAS). Measurements at around  $0^\circ$  were performed by operating the spectrometer in overfocused mode [17] and by stopping the beam at a Faraday cup placed inside the first dipole magnet of the Grand Raiden spectrometer. The Faraday cup was also used to integrate the current of the beam.

test of effective interactions employed in nuclear shell models.

The experiment was conducted using the Grand Raiden high-resolution spectrometer (see Fig. 1) at the Research Center for Nuclear Physics of Osaka University (Japan) [16]. The aim of the experiment was to measure absolute differential cross sections with a high precision. We performed systematic measurements in normal kinematics, namely,  $^{24}\text{Mg}(^3\text{He}, p)^{26}\text{Al}$ ,  $^{24}\text{Mg}(p, ^3\text{He})^{22}\text{Na}$ ,  $^{28}\text{Si}(p, ^3\text{He})^{26}\text{Al}$ ,  $^{40}\text{Ca}(p, ^3\text{He})^{38}\text{K}$ , and  $^{32}\text{S}(^3\text{He}, p)^{34}\text{Cl}$ . The thickness of the targets, around  $300 \mu\text{g}/\text{cm}^2$ , was chosen to minimize the straggling and achieve an excitation energy resolution below 70 keV (FWHM) for all the measurements listed above. The azimuthally varying field cyclotron delivered  $^3\text{He}$  and  $p$  beams at 25 and 65 MeV, respectively, with an intensity of around 50 pA. These energies are appropriate due to the momentum matching for these reactions where the transitions to  $0^+$  and  $1^+$  are possible with  $L = 0$  and  $L = 2$  angular momenta.

Outgoing proton/ $^3\text{He}$  particles were momentum-analyzed by the Grand Raiden spectrometer (see Fig. 2). The position of these particles in the focal plane was determined using two multiwire drift chambers of the vertical drift type. Identification of the particles was done by measuring the time of flight and the energy loss of the particles in the focal plane using a plastic scintillator. Particles were detected from  $0^\circ$  up to  $30^\circ$  (at  $2^\circ$  intervals) using a magnetic setting that allowed us to measure up to 3 MeV of excitation energy. For angles below  $6^\circ$ , the spectrometer was operated in overfocused mode [17]. The target thickness was also monitored during the experiment by detecting elastically scattered proton/ $^3\text{He}$  particles at  $60^\circ$  in the focal plane of the large acceptance spectrograph. The angular distributions were compared to calculations performed with well-known optical potentials, as discussed later, to infer the thickness of the target.

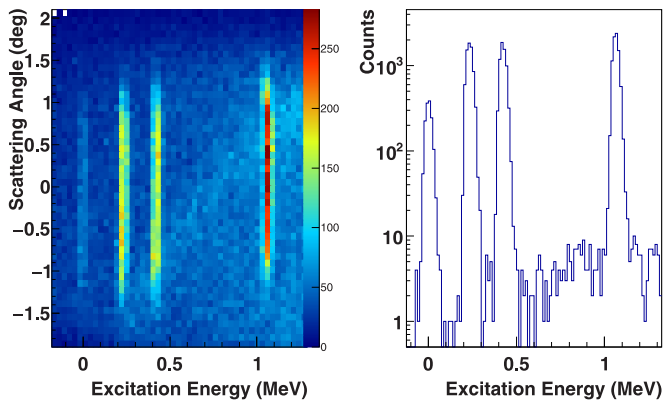


FIG. 2. Left: Excitation energy spectrum as a function of the scattering angle for the  $^{24}\text{Mg}(^3\text{He},p)^{26}\text{Al}$  reaction. The spectrum is gated on protons. The  $^{26}\text{Al}$  states can be unambiguously identified: 0.0 MeV ( $5^+$ ), 0.228 MeV ( $0^+$ ), 0.416 MeV ( $3^+$ ), and 1.06 MeV ( $1^+$ ). Right: Same as the left panel, but projected onto the excitation energy axis.

In order to understand the underlying reaction mechanism, we have performed second-order distorted-wave Born approximation (DWBA) calculations with the code FRESKO [18,19], which should account properly for the reaction mechanism at the energies used in this work. In second-order DWBA, two contributions interfere in order to create the total transfer cross section: simultaneous and sequential transfer. On top of that, there is another contribution arising from nonorthogonality terms, which we avoid here by choosing the *prior-post* form for the sequential term [18]. The correct assessment of the three terms and their interference is expected to quantitatively reproduce the full transfer cross section without using any “unhappiness” factor as has been shown in recent cases [20–22]. To the best of our knowledge, this is the first time that second-order DWBA calculations have been applied to  $np$  transfer. This new framework provides valuable insight into the determination of whether a structure model successfully predicts the  $np$  pairing and, more importantly, the relative importance between the  $T = 0$  and the  $T = 1$  possibilities.

The wide variety of optical potentials introduces an additional dimension of uncertainty. However, the ratio of the cross section populating the  $0^+$  to the one populating the  $1^+$  should not strongly depend on the selected optical potential as long as one uses the same one in both calculations. We have kept the same family of optical potentials for the different counterparts of all the reactions. For all of the reactions, the best overall agreement is found when using Menet for protons, Lohr-Haerberli for deuteron potentials, and Bechetti-Greenlees for  $^3\text{He}$  potentials [23]. Other options have been explored leading to important variations in the cross section at  $0^\circ$ . However, these differences are considerably reduced if we consider only those combinations of optical potentials that produce an angular distribution consistent with the experimental data. These differences are also smaller in the ratios as expected, although they can still be important. Therefore, we have checked that these variations do not affect the present conclusions. In particular, the  $^{32}\text{S}(^3\text{He},p)^{34}\text{Cl}$  case is the only one here whose ratio is affected by the choice

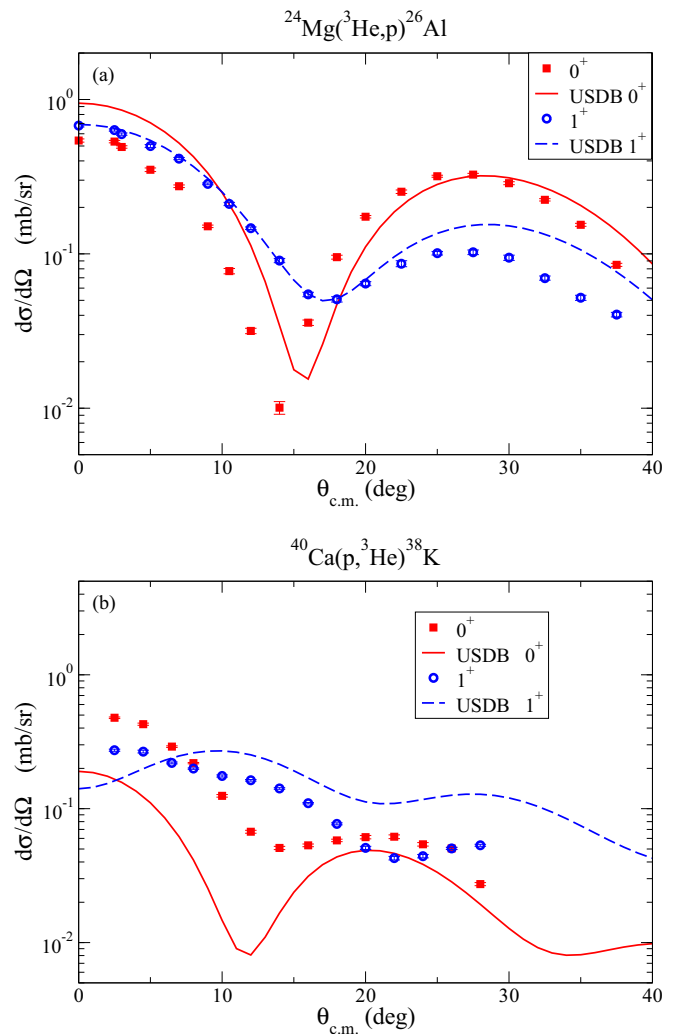


FIG. 3. Cross sections for (a)  $^{24}\text{Mg}(^3\text{He},p)^{26}\text{Al}$  and for (b)  $^{40}\text{Ca}(p,^3\text{He})^{38}\text{K}$  for the  $np$  transfer to the first  $0^+$  and first  $1^+$  states. We make comparisons with the second-order DWBA calculations (see text). Uncertainties are smaller than the symbols representing the data for some angles.

of the optical potential. Details of the impact from different choices of optical model parameters will be presented in a longer follow-up paper.

The overlaps of the  $sd$ -shell nuclei studied were constructed from two-nucleon spectroscopic amplitudes calculated with wave functions obtained from the USDB (universal  $sd$ -shell interaction B) [24] Hamiltonian using the shell-model code NUSHELLX [25]. The USDB is a phenomenological interaction specifically fitted to reproduce the spectrum of nuclei in the  $sd$  shell. For the sequential part of the transfer reaction we make an intermediate state factorization of the two-nucleon amplitude into two terms. This division is arbitrary but the result is insensitive to this change provided that the total form factor is consistent with the two-nucleon amplitude. The energy of the intermediate state is defined as half the energy difference between initial and final states. We show the results for the  $^{24}\text{Mg}(^3\text{He},p)^{26}\text{Al}$  reaction in Fig. 3(a) and those for the  $^{40}\text{Ca}(p,^3\text{He})^{38}\text{K}$  reaction in Fig. 3(b). For the

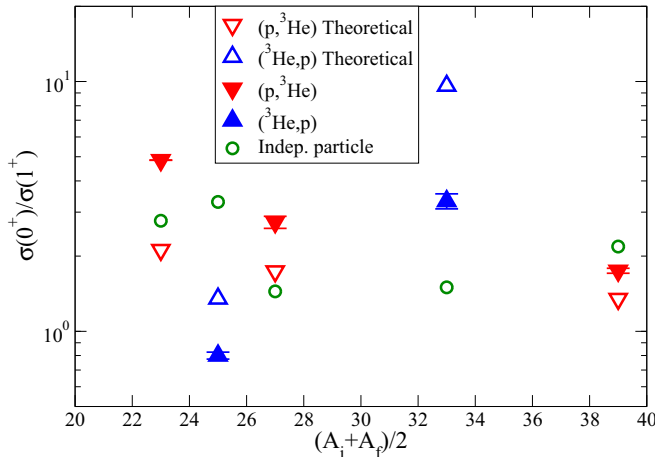


FIG. 4. Experimental ratios (filled triangles) between the transfer cross sections to the  $0^+$  and the  $1^+$  states in the final nuclei, measured at the smallest angle possible in each case. The abscissa is the half-sum of the initial and final mass numbers of the nuclei of interest. Triangles indicate  $({}^3\text{He}, p)$  reactions, whereas inverted triangles represent  $(p, {}^3\text{He})$  reactions. We also include the corresponding theoretical ratios, represented by open symbols. Open triangles correspond to the ratio calculated with the USDB spectroscopic factors, and open green circles, to the ratio calculated by assuming independent particles without pairing (see text).

former, the theoretical predictions overestimate the  $T = 1$  case but indicate a good agreement for the  $T = 0$  case. Different results were reported in Ref. [26], indicating a systematic underestimation of the  $T = 0$   $np$  pair removal cross section in the  $p$  shell. This calculation is similar to the more standard  $(t, p)$  case for  $T = 1$ . For the  $T = 0$  case, the  $L = 0$  and  $L = 2$  components are mixed. Both contributions can be determined with these calculations, with the  $L = 0$  component dominant at small angles. In this way, it is possible to estimate the relative strength of correlations in  $T = 0$  and  $T = 1$  through the ratio of the cross sections. The present calculation can also be used to estimate the uncertainty of this ratio for those cases where measuring at  $0^\circ$  has not been possible.

For the  ${}^{40}\text{Ca}(p, {}^3\text{He}){}^{38}\text{K}$  reaction, the agreement in magnitude is less satisfactory than in the previous case. We have to keep in mind that  ${}^{40}\text{Ca}$  is at the end of the  $sd$  shell and is therefore a double-magic nucleus. For this reaction, we do not include here  $f$  orbitals, which might contribute to the total cross section, improving the present results. The theoretical ratio between the cross sections of the  $0^+$  and the  $1^+$  states at around  $0^\circ$  is underestimated (1.35 instead of 1.75), and the angular distribution is not perfectly reproduced. However, we believe that these results open up promising perspectives considering that the components from the  $fp$  shell are not included.

In general, good agreement is found overall between the measurement and the theoretical calculations for the shape and magnitude of the different reactions studied. However, this agreement does not translate into a satisfactory reproduction of the trend of the experimental ratios. Figure 4 shows the ratio between the transfer cross sections of the  $0^+$  and the  $1^+$  states in the final nuclei, measured at the smallest angle possible in each case. On the abscissa we have chosen the

half-sum of the initial and final mass number of the nuclei of interest. This selection is based on the fact that a hypothetical  $A({}^3\text{He}, p)A + 2$  from a  $0^+$  ground state to a  $0^+$  ground state will yield the same cross section as the inverse reaction  $A + 2(p, {}^3\text{He})A$ . With the present selection of the abscissa, both cross sections will coincide in the plot for an  $x$  value of  $A + 1$ . Theoretical calculations for the same ratios are also shown in Fig. 4 by open symbols. These theoretical ratios have always been calculated for  $0^\circ$ .

The experimental ratios do not show a clear trend with the number of valence particles. However, if we compare these ratios with the independent particle limit (open green circles in Fig. 4), we see how the deviation from this reference line increases. The estimation of this independent particle may differ from previous calculations [15]. This is due to the fact that we performed full second-order DWBA calculations taking into account a zero admixture for the wave functions which includes the proper  $Q$  values. We found these independent particle ratios to depend on the different  $Q$  values and also on the component for the pure wave function. In this regard, we have chosen the dominant component in the shell-model calculation, i.e.,  $(d_{5/2})^2$  for the first three reactions and  $(d_{3/2})^2$  for the latter two. This independent particle limit always underestimates the transfer cross section, since it does not include any pairing. Even a small amount of the latter will increase the cross section. When comparing the ratios, if the experimental value is above (or below) the single-particle limit, we can infer that the  $T = 1$  (or  $T = 0$ ) pairing is dominant over the other one.

For some cases, the deviation shows a dominance of the cross section populating the  $1^+$  state, thus supporting the idea of a strong  $T = 0$   $np$  pairing. Compared with the shell-model calculation, the USDB interaction seems to overestimate this deviation. For the  ${}^{40}\text{Ca}(p, {}^3\text{He}){}^{38}\text{K}$  case we see that the single-particle ratio is pretty close to the experimental point as expected for a doubly magic nucleus. However, the sole single-particle cross section does not fully reproduce the experimental one for either of the two cases. There is room for a little enhancement, which in any case is compatible with the possible treatment of this case as a vibration in  ${}^{40}\text{Ca}$ .

The collective nature of the  $T = 0$   $np$  pairing can be understood theoretically by looking at how the different parts of the  $np$  wave function contribute to the final cross section. In an  $nn$  superfluid nucleus, all the components interfere constructively with the transfer from ground state to ground state, thus creating a characteristic large enhancement of the cross section. In Fig. 5, we show the calculations for the transfer of an  $np$   $L = 0$  pair to the first  ${}^{26}\text{Al}$   $1^+$  state where we have included the different parts of the overlap. Considering only the part of the neutron and the proton in the  $d_{5/2}$  wave, we see that each additional term consistently increases the total cross section, especially at  $0^\circ$ . It is necessary to add almost all the components in order to reproduce the experimental data. Figure 5 also shows that there is a nonnegligible enhancement resulting from parts of the overlap where the neutron and the proton are not in the same state. In other words, the  $(d_{5/2})(d_{3/2})$  component increases the cross section even at  $0^\circ$ , and therefore, it is needed in order to explain the ratio shown in Fig. 4. This component does not appear in the  $nn$  (or  $pp$ ) BCS Cooper

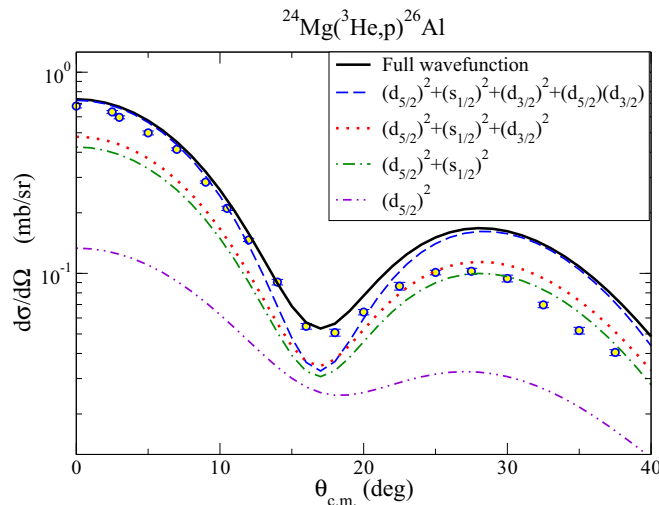


FIG. 5. Cross sections for  $^{24}\text{Mg}(^3\text{He}, p)^{26}\text{Al}$  for the first  $1^+$  state. Uncertainties are smaller than the symbols representing the data. The different lines correspond to the theoretical calculations for transferring  $L = 0$  pairs but adding up different parts of the overlap to recover the full overlap ( $^{24}\text{Mg}(0^+)^{26}\text{Al}(1^+)$ ). The corresponding theoretical spectroscopic factor for each part of the wave function is omitted in the legend but considered in the calculation.

pair. However, the  $(d_{5/2})(d_{3/2})$  component is perfectly allowed in the case of  $T = 0$  and has to be taken into account when generalizing BCS for  $np$  pairing.

In conclusion, we have established a novel analysis framework that improves our understanding of the  $np$  pairing phenomena in other systems and helps to elucidate whether the isoscalar pairing force interaction is present. In order to shed some light on the nature of the  $T = 0$  isoscalar  $np$  pairing, we performed a series of systematic  $np$  transfer measurements on  $sd$ -shell  $N = Z$  nuclei. These high-quality data were taken under identical conditions to avoid systemic uncertainties, spanning a wide angular distribution, from close

to  $0^\circ$  up to  $30^\circ$ . We obtained the absolute differential cross sections with a high precision and thus the ratio between the cross sections  $\sigma(0^+)/\sigma(1^+)$ . In order to understand how the cross-section ratio relates to the relative strength between the isoscalar and the isovector pairing modes, we performed second-order DWBA calculations taking into account shell-model calculations with the USDB interaction. We found a satisfactory agreement for the shape of the distribution but not for the absolute comparison of the ratios. With the help of these second-order DWBA calculations we can make comparisons with the ratios for pure or zero-pairing wave functions. From these, we find cases in which the  $T = 0$  pairing appears to dominate over the traditional or more standard  $T = 1$  channel. We have also shown how the different components contribute coherently to increase the cross section in one of these particular cases:  $^{24}\text{Mg}(^3\text{He}, p)^{26}\text{Al}(1^+)$ . In addition, the results indicate that the cross sections to the  $1^+$  are dominated by the transfer of an  $L = 0$  pair as in the  $T = 1$  pairing. However, certain components with a nonnegligible contribution to this  $L = 0$  transfer are not included in the typical Cooper pair [5]. Building on this foundational work, new and follow-up experiments with radioactive beams are required to further our understanding of the evolution of  $np$  pairing correlations along the  $N = Z$  line. Such challenging experiments will be available at future rare-isotope facilities capable of providing high-intensity proton-rich beams.

The authors thank the RCNP ring cyclotron staff for delivering the high-quality proton and  $^3\text{He}$  beams. The research leading to these results received funding from the European Commission Seventh Framework Programme (FP7/2007-2013) under Grant Agreement No. 600376. J.A.L. was a Marie Curie Piscopia fellow at the University of Padova. B.A.B. acknowledges support from NSF Grant No. PHY-1404442. This material is based upon work supported by the US Department of Energy, Office of Science, Office of Nuclear Physics, under Contract No. DE-AC02-05CH11231 (LBNL).

- [1] D. Brink and R. Broglia, in *Nuclear Superfluidity: Pairing in Finite Systems (Cambridge Monographs on Particle Physics, Nuclear Physics and Cosmology)* (Cambridge University Press, Cambridge, UK, 2005).
- [2] S. Frauendorf and A. O. Macchiavelli, *Prog. Part. Nucl. Phys.* **78**, 24 (2014).
- [3] G. Martinez-Pinedo, K. Langanke, and P. Vogel, *Nucl. Phys. A* **651**, 379 (1999).
- [4] Y. Lei, S. Pittel, N. Sandulescu, A. Poves, B. Thakur, and Y. M. Zhao, *Phys. Rev. C* **84**, 044318 (2011)
- [5] G. F. Bertsch and Y. Luo, *Phys. Rev. C* **81**, 064320 (2010)
- [6] A. L. Goodman, *Adv. Nucl. Phys.* **11**, 263 (1979)
- [7] A. Gezerlis, G. F. Bertsch, and Y. L. Luo, *Phys. Rev. Lett.* **106**, 252502 (2011)
- [8] A. O. Macchiavelli *et al.*, *Phys. Lett. B* **480**, 1 (2000).
- [9] K. Yoshida, *Phys. Rev. C* **90**, 031303(R) (2014).
- [10] P. Fröbich, *Phys. Lett. B* **37**, 338 (1971).
- [11] P. Van Isacker, D. D. Warner, and A. Frank, *Phys. Rev. Lett.* **94**, 162502 (2005).
- [12] R. M. Del Vecchio *et al.*, *Nucl. Phys. A* **265**, 220 (1976).
- [13] N. Takahashi, Y. Hashimoto, Y. Iwasaki, K. Sakurai, F. Soga, K. Sagara, Y. Yano, and M. Sekiguchi, *Phys. Rev. C* **23**, 1305 (1981).
- [14] S. H. Nann *et al.*, *Nucl. Phys. A* **198**, 11 (1972).
- [15] A. O. Macchiavelli *et al.*, in *ANL Physics Division Annual Report ANL-03/23* (Argonne National Laboratory, Lemont, IL, 2002), p. 21.
- [16] M. Fujiwara *et al.*, *Nucl. Instrum. Methods* **422**, 484 (1999).
- [17] H. Fujita *et al.*, *Nucl. Instrum. Methods* **469**, 55 (2001).
- [18] I. J. Thompson, in *50 Years of Nuclear BCS*, edited by R. A. Broglia and V. Zelevinsky (World Scientific, Singapore, 2013), chap. 34.
- [19] I. J. Thompson, *Comput. Phys. Rep.* **7**, 167 (1988).
- [20] G. Potel, F. Barranco, F. Marini, A. Idini, E. Vigezzi, and R. A. Broglia, *Phys. Rev. Lett.* **107**, 092501 (2011); **108**, 069904(E) (2012).
- [21] I. Tanihata, M. Alcorta, D. Bandyopadhyay, R. Bieri, L. Buchmann, B. Davids, N. Galinski, D. Howell, W. Mills, S.

- Mythili, R. Openshaw, E. Padilla-Rodal, G. Ruprecht, G. Shiffer, A. C. Shoter, M. Trinczek, P. Walden, H. Savajols, T. Roger, M. Caamano, W. Mittig, P. Roussel-Chomaz, R. Kanungo, A. Gallant, M. Notani, G. Savard, and I. J. Thompson, *Phys. Rev. Lett.* **100**, 192502 (2008).
- [22] K. Wimmer, T. Kröll, R. Krücken, V. Bildstein, R. Gernhäuser, B. Bastin, N. Bree, J. Diriken, P. Van Duppen, M. Huyse, N. Patronis, P. Vermaelen, D. Voulot, J. Van de Walle, F. Wenander, L. M. Fraile, R. Chapman, B. Hadinia, R. Orlandi, J. F. Smith, R. Lutter, P. G. Thierolf, M. Labiche, A. Blazhev, M. Kalkühler, P. Reiter, M. Seidlitz, N. Warr, A. O. Macchiavelli, H. B. Jeppesen, E. Fiori, G. Georgiev, G. Schrieder, S. D. Gupta, G. Lo Bianco, S. Nardelli, J. Butterworth, J. Johansen, and K. Riisager, *Phys. Rev. Lett.* **105**, 252501 (2010).
- [23] C. M. Perey and F. G. Perey, *Atom. Data Nucl. Data Tables* **17**, 1 (1976).
- [24] B. A. Brown and W. A. Richter, *Phys. Rev. C* **74**, 034315 (2006).
- [25] B. A. Brown and W. Rae, *Nucl. Data Sheets* **120**, 115 (2014).
- [26] E. C. Simpson and J. A. Tostevin, *Phys. Rev. C* **83**, 014605 (2011).